International Symposium
On Turbulence and Shear Flow
Phenomena (TSFP-9)
June 30 - July 3, 2015 *Melbourne, Australia*

EFFECT OF LOCAL FLOW CONTROL ON TRANSITION IN A LAMINAR SEPARATION BUBBLE

Serhiy Yarusevych
Department of Mechanical and Mechatronics Engineering
University of Waterloo
200 University Ave. W, Waterloo, Ontario, Canada, N2L 3G1
syarus@uwaterloo.ca

Marios Kotsonis
Faculty of Aerospace Engineering
Delft University of Technology
Kluyverweg 1, Delft, The Netherlands, 2629HS
m.kotsonis@tudelft.nl

ABSTRACT

This work examines the effect of active flow control on stability and transition in a laminar separation bubble forming on an airfoil. Experiments are performed in a wind tunnel facility on a NACA 0012 airfoil at a chord Reynolds number of 130,000 and at an angle of attack of 2 degrees. Controlled disturbances are introduced upstream of a laminar separation bubble forming on the suction side of the airfoil using a surface-mounted Dielectric Barrier Discharge plasma actuator. Planar, time-resolved Particle Image Velocimetry is used to characterise the flow field. The effect of frequency and amplitude of introduced disturbances on flow development is examined. It is shown that excitation can lead to significant changes in separation bubble topology and the characteristics of coherent structures formed in the aft portion of the bubble. Statistical, topological and linear stability theory analysis demonstrate that significant mean flow deformation produced by controlled disturbances does not necessarily lead to substantial changes in stability characteristics compared to that in unforced baseline case. The findings provide a new outlook on the role of controlled disturbances in separated shear layer transition and instruct the development of effective flow control strategies.

INTRODUCTION

A Laminar Separation Bubble (LSB) is a characteristic feature of flow development over an airfoil at low chord Reynolds numbers (Re_c) below approximately 500,000 (e.g., Carmichael (1981)). It typically forms on the suction side of an airfoil due to laminar boundary layer separation, followed by separated shear layer transition and subsequent reattachment. In general, the airfoil performance degrades in the low Reynolds number domain, and the degree of performance degradation largely depends on the characteristics of the laminar separation bubble (e.g., Gaster (1967); Carmichael (1981)). Consequently, significant research efforts have been directed towards gaining an improved understanding of flow phenomena within separation bubbles (e.g., Dovgal *et al.* (1994); Burgmann & Schroeder (2008); Hain *et al.* (2009); Jones *et al.* (2010); Marxen & Henningson (2011)) and developing effective flow control strategies (e.g., Gad-el Hak (2001); Yarusevych *et al.* (2007); Postl *et al.* (2011); Marxen *et al.* (2015)).

Early studies (e.g., Tani (1964); Gaster (1967)) have provided a comprehensive description of the time-averaged separation bubble topology. Subsequently, significant advancements have been made towards a comprehensive characterisation of separated shear layer transition (e.g., Marxen & Henningson (2011); Boutilier & Yarusevych (2012)). It has been shown that the transition process begins with the amplification of small amplitude disturbances in the separated shear layer. The initial amplification is associated with a band of unstable frequencies and is well modelled by linear stability theory (Boutilier & Yarusevych (2012)). The process is largely governed by a convective, inviscid Kelvin-Helmholtz instability. However, Alam & Sandham (2000) have demonstrated that an absolute instability can also manifest in the separated shear layer when it is bound by a strong reverse flow region near the wall. This requires maximum reverse flow velocities to reach approximately 15% of the edge velocity, which is uncommon in separation bubbles investigated experimentally. The later stages of transition in the separated shear layer are governed by non-linear interaction between the disturbances, and the continuous growth of disturbance amplitude leads to separated shear layer roll-up and periodic shedding of shear layer vortices in the aft portion of the bubble (e.g., Marxen *et al.* (2013)). These structures are argued to be responsible for producing time-averaged flow reattachment (e.g., Jones *et al.* (2010)).

The key role played by the transition process in the development of separation bubbles makes these flows sensitive to the level of background disturbances in experimental facilities (e.g., Ol. et al, 2005) and numerical simulations (e.g., Marxen & Henningson (2011)). It also enables the implementation of active flow control strategies that can impact LSB characteristics and improve airfoil performance. Periodic excitation using external acoustic waves (e.g., Yarusevych *et al.* (2007)), embedded synthetic jets

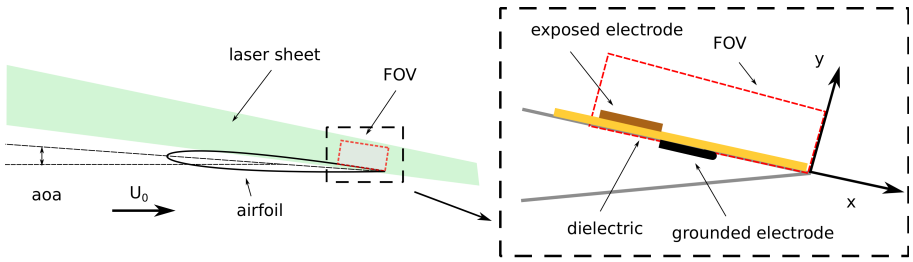

Figure 1. Experimental setup.

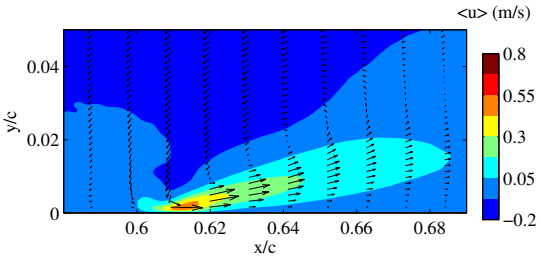

Figure 2. Time-averaged flow field induced by the actuator operated continuously at carrier frequency of 5000 Hz and voltage of 5 kV_{pp} in quiescent conditions.

(e.g., Greenblatt & Wygnanski (2000)), and plasma-based actuators (e.g., Rizzetta & Visbal (2011)) have been considered and shown to be capable of inducing flow reattachment on an airfoil exhibiting separation. The effectiveness of the control depends strongly on the amplitude and the frequency of excitation. Using controlled acoustic excitation, Yarusevych *et al.* (2007) have identified a link between the most effective excitation frequency and that of the most amplified disturbances in undisturbed flow. Marxen & Henningson (2011) and Marxen *et al.* (2015) considered the effect of controlled disturbances on the development of a separation bubble in direct numerical simulations. Their results show that the introduction of flow perturbations changes the topology of the bubble, implying that flow excitation also influences stability characteristics of the laminar separation bubble.

The present work investigates experimentally the response of LSBs to local disturbances introduced by a Dielectric Barrier Discharge (DBD) plasma actuator. The goal is to investigate the spatio-temporal response of the bubble to disturbances and to study the effect of the associated changes in the flow topology on stability and transition in the separated shear layer.

EXPERIMENTAL SETUP

The experiments were performed in a vertical low-speed open jet facility (v-tunnel) at Delft University of Technology. The wind tunnel is capable of maximum velocities of 40 m/s, while the large contraction ratio and anti-turbulence screens ensure freestream turbulence levels below 0.1 %. A polycarbonate NACA 0012 airfoil model, with a chord length of 200 *mm* and a span of 400 *mm*, was placed about 150 *mm* downstream of the circular open-jet nozzle (Fig.1). Circular transparent polycarbonate side plates of diameter 300 *mm* were placed on the sides of the airfoil in order to ensure flow two-dimensionality and allow for optical access. The boundary layer on the pressure side of the airfoil was tripped using a strip of randomly distributed three-dimensional roughness elements (carborundum, nominal grain size of 0.36 *mm*). This was done in order to prevent the formation of a separation bubble on the pressure side and the associated shedding of coherent structures over the trailing edge, which can produce tonal noise emissions and affect the dynamics of the LSB on the suction side (Pröbsting *et al.* (2014)).

Time-resolved, planar, two-component Particle Image Velocimetry (PIV) system was comprised of a LaVision Imager Pro HS 4M high speed CMOS camera (1.3kHz at 4Mpx, 11μm pixel pitch) and a Quantronix Darwin-Duo Nd:YLF laser (30 *mJ* per pulse), which were synchronised using a LaVision High-Speed controller and Davis 8 software package. The flow was seeded using non-toxic water-glycol particles with an average diameter of 1μm. The particles were illuminated at the mid span of the airfoil model by a light sheet of about 2 *mm* in thickness. The camera was equipped with a Nikon Micro-Nikkor 105 *mm* objective with aperture number ($f\#$) set to 5.6. The imaged field of view (FOV) was approximately 90 $\times$ 19 *mm*, with a magnification factor of approximately 0.25. The camera sensor was cropped to 2016 $\times$ 428 pixels and image pairs were recorded at 2 kHz. The acquired image sequences were analysed using a multi-grid, multi-pass correlation algorithm in Davis 8. The final interrogation window size was 16 $\times$ 16 pixels, with 75% overlap, resulting in a vector density of 5.6 vectors per *mm*.

Flow control was performed by means of a DBD plasma actuator. The actuator was constructed using two thin self-adhesive copper electrodes of 30 μm thickness, separated by polyimide dielectric (Kapton®) of 110 μm thickness, directly attached to the surface of the suction side of the airfoil (Fig.1). The exposed electrode was powered using a TREK 20/20C High-Voltage (HV) amplifier, while the covered electrode was grounded. Both electrodes were 10 *mm* wide in the streamwise direction and 120 *mm* in the spanwise direction. The actuator was placed 120 *mm* from the leading edge (at x/c = 0.6), just upstream of laminar boundary layer separation.

The plasma actuator was characterised in quiescent environment and a representative time-averaged velocity field is depicted in Fig.2, pertaining to continuous excitation at carrier frequency of 5000 Hz and applied voltage of 5 kV_{pp}. In agreement with Kotsonis & Ghaemi (2011), the actuator produces a micro-jet, aligned at an angle to the surface and oriented in the general direction of the free stream. The time-resolved data showed that the velocity of the jet fluctuates periodically, following the fluctuations in the excitation voltage. For the performed experiments the actuator was operated in continuous or pulsed mode. For continuous

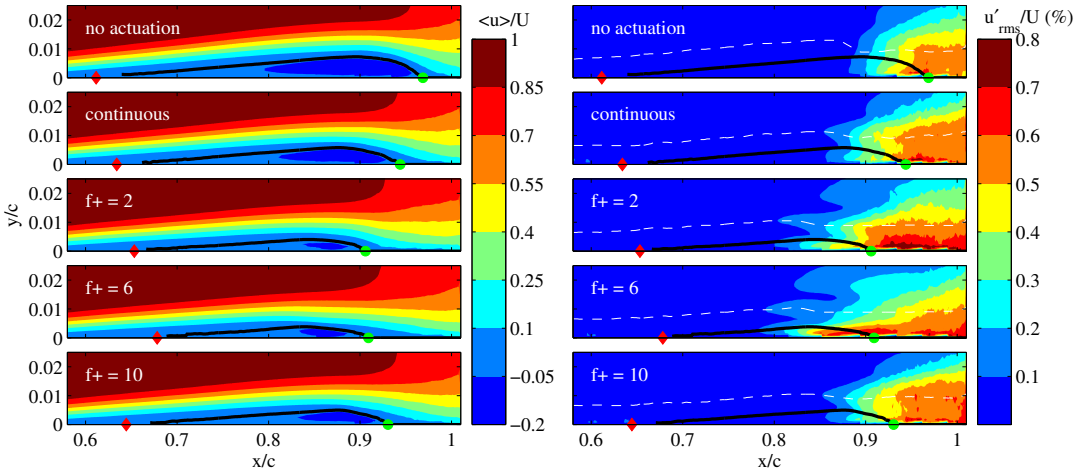

Figure 3. Mean and rms streamwise velocity contours for a range of excitation frequencies. For the controlled cases, the actuation is applied at 3.5 kV_{pp}. Solid black lines mark the dividing streamlines. Dashed lines mark the locus of maximum rms values in the streamwise direction. Red diamonds denote the separation points while green circles denote the reattachment points.

operation the AC frequency of applied voltage was fixed at 5 kHz. For pulsed mode, square wave modulation of the excitation voltage was used to introduce periodic disturbances at a desired frequency (effectively switching the actuator on and off). The carrier frequency of 5000 Hz was used, which is an order of magnitude higher than the highest frequency of interest in the flow investigated. The modulations were applied at frequencies (f) from 100 Hz to 500 Hz (reduced frequency $f+ = f \cdot c/U$ varied from 2 to 10 respectively), which corresponds to a range of unstable frequencies in the undisturbed separation bubble, and amplitudes ranging from 3 kV_{pp} to 5 kV_{pp}. For a given voltage amplitude, the duty cycle was adjusted for each modulation frequency to yield the same energy input per pulse across the investigated range of frequencies. The maximum jet velocity induced by the actuator is estimated to vary from 0.2 to 1 m/s for the range of applied voltage used in this study.

RESULTS

All experiments were performed at $\alpha = 2^\circ$ and Re_c = 130,000. The parametric tests considered the response of the laminar separation bubble to controlled disturbances in a range of excitation amplitudes and frequencies around the natural frequency of the most amplified disturbances in an unperturbed flow. Fig.3 depicts the mean and root-mean-square (RMS) streamwise velocity contours for a range of actuation parameters. For the baseline case (no actuation) the results show the presence of a laminar separation bubble on the suction side of the airfoil, extending from x/c = 0.62 to x/c = 0.97 (Fig.3, top). When disturbances are introduced at a constant actuation amplitude of 3.5 kV_{pp}, the extent of the bubble is diminished; however, the effect depends significantly on the excitation frequency. For the excitation applied continuously at the carrier frequency (5000 Hz), a moderate decrease in bubble length is observed, with both separation and reattachment locations being affected. However, the effect becomes more pronounced when the actuator is modulated at lower frequencies. The most pronounced effect is observed at $f+ = f \cdot c/U = 6$ ($f = 300Hz$), suggesting the existence of optimal modulation frequency in terms of bubble size. The RMS contours in Fig.3 show that the observed changes in the position and extent of the separation bubble are linked to the increase in the amplitude of disturbances in the separated shear layer, with velocity fluctuations attaining notably higher amplitudes at a given streamwise location when excitation is applied. This implies that actuation advances transition in the separated shear layer, which not only induces earlier time-averaged reattachment but also time-averaged parameters of the separation bubble with excitation frequency and amplitude, respectively. The data in Fig.4 shows that the bubble reaches its minimum extent at $f+ \approx 6$. When the excitation is applied at this frequency, the increase in excitation amplitude leads to a continuous diminishment of the separation bubble, with separation being delayed and reattachment occurring farther upstream (Fig.5). The observed effect of excitation amplitude on the characteristics of the separation bubble is similar to that reported by Yarusevych *et al.* (2007) for external acoustic excitation.

The spectral content of disturbances amplified in the separated shear layer can be assessed using the power spectral density (PSD) contours of streamwise velocity fluctuations shown in Fig.6. For the baseline case, the packet of amplified disturbances is seen at frequencies within approximately $5 < F+ < 10$, with disturbances associated with $F+ \approx 6$ reaching higher amplitudes at a given upstream location. Evidently, the optimal excitation frequency $f+ \approx 6$ (f = 300 Hz) identified in Fig.4 is associated with the frequency of the most amplified disturbances in the baseline flow. The results in Fig.6 illustrate that, when the excitation is applied at a particular frequency, the frequency of the most amplified disturbances in the shear layer locks to the excitation frequency, its harmonics and a sub-harmonic. The most profound amplification is attained, however, when the excitation frequency (or its harmonic) matches that of the most unstable disturbances in the undisturbed flow. This advances flow transition, which is marked by the rapid broadening of the energy content across a wide range of frequencies in Fig.6, and leads to significant changes in separation bubble characteristics seen in Figs.3 and 4. The results also illustrate the significance of harmonics amplifica-

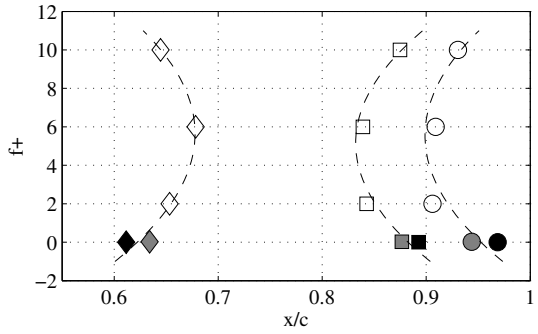

Figure 4. The effect of excitation frequency on the location of laminar separation (◊), maximum bubble height (□), and reattachment (◯). Black symbols denote baseline case while grey symbols denote continuous actuation $A = 3.5kV_{pp}$ (fitted trends are second-order polynomials).

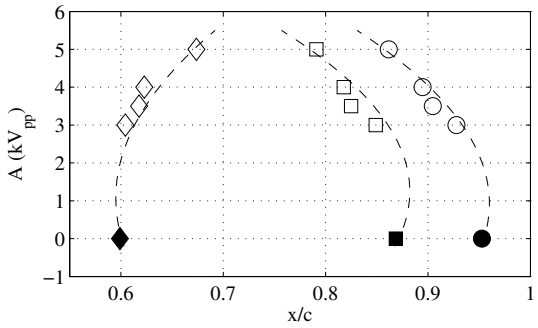

Figure 5. The effect of excitation amplitude on the location of laminar separation (◊), maximum bubble height (□), and reattachment (◯). Black symbols denote baseline case. $f+ = 6$ (fitted trends are second-order polynomials).

tion when such harmonics fall within a range of unstable frequencies in the baseline flow. Specifically, for $f+ = 2$, the first and second harmonics fall within the unstable frequency range and are strongly amplified. In contrast, for $f+ = 10$, a less significant amplification at the excitation frequency and its sub harmonic is attained. As a consequence, while both excitation frequencies are equally separated from the fundamental frequency $F+ = 6$, excitation at $f+ = 2$ leads to a more significant diminishment of the separation bubble compared to that at $f+ = 10$ (e.g., Fig.3).

The changes brought about by the controlled disturbances to spatio-temporal dynamics of the laminar separation bubble are illustrated in Fig.7, which depict a series of instantaneous vorticity contours for the baseline and controlled case at $f+ = 6$. The results show that the separated shear layer rolls up into periodic vortical structures upstream of the mean reattachment location. These structures facilitate the entrainment of higher momentum fluid, which leads to unsteady flow reattachment. Specifically, the position of the instantaneous reattachment location fluctuates substantially during each shedding cycle around the mean position seen in Fig.3. For the baseline case, the average frequency of the shedding is $F+ \approx 6$, approximately matching the most amplified frequency in the separated shear layer (Fig.6). Applying the excitation at $f+ = 6$ promotes transition and locks the amplified frequency band to the excitation frequency, which leads to earlier and more coherent shedding in the aft portion of the separation bubble than that seen for the baseline case.

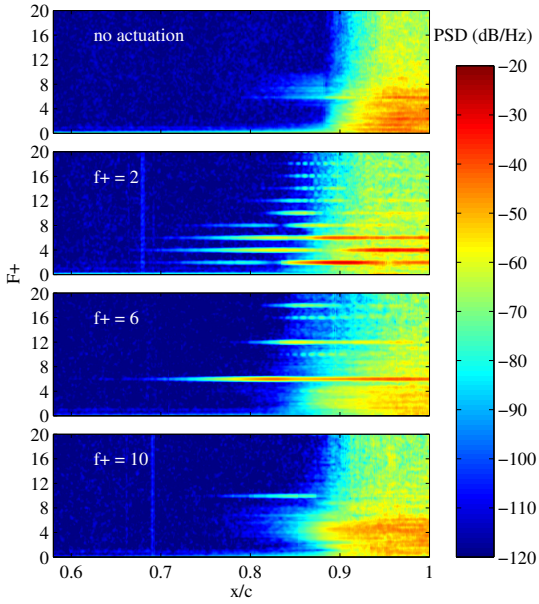

Figure 6. Spectra of streamwise velocity fluctuations measured in the core of the separated shear layer (dashed line in Fig.3). For the controlled cases, the actuation is applied at 3.5 kV_{pp}. $(F+ = F \cdot c/U)$

Dashed lines in Fig.7 trace the streamwise positions speed, and it remains nearly constant for the baseline and the controlled cases. The wavelength of the vortices also remains approximately constant, as expected for the nearly matching shedding frequencies. The results in Fig.3 suggest that the roll-up vortices lose coherence and start to breakdown in the redeveloping turbulent boundary layer, which is evidenced by the appearance of the opposite sign vorticity in the core of these strictures. However, for the controlled case, this process is delayed. Also, the cores of the vortices in the controlled case exhibit strong streamwise deformations, attaining notable elliptic shapes prior to breakup. Based on the numerical results of Marxen *et al.* (2013), this indicates that the breakup mechanism can differ between the baseline and controlled cases.

The foregoing discussion shows that the optimal frequency of controlled disturbances correlates with the fundamental frequency of the amplified natural disturbances in unexcited flow. At the same time, excitation at optimal frequency leads to significant deformation of the mean flow field (Fig.3). Marxen & Henningson (2011) argue that such deformations can lead to changes in stability characteristics, which, if significant, would lead to changes in optimal excitation parameters. To investigate this further, linear stability theory (LST) analysis was applied. The Orr-Sommerfeld equation was solved assuming convective amplification of small amplitude disturbances in the separated shear layer using measured mean velocity profiles (Van Ingen & Kotsonis (2011)). Note that the convective nature of the disturbance amplification is consistent with the experimental measurements, and the maximum reverse flow velocities are lower than the threshold required for the occurrence of a global instability (Alam & Sandham (2000)).

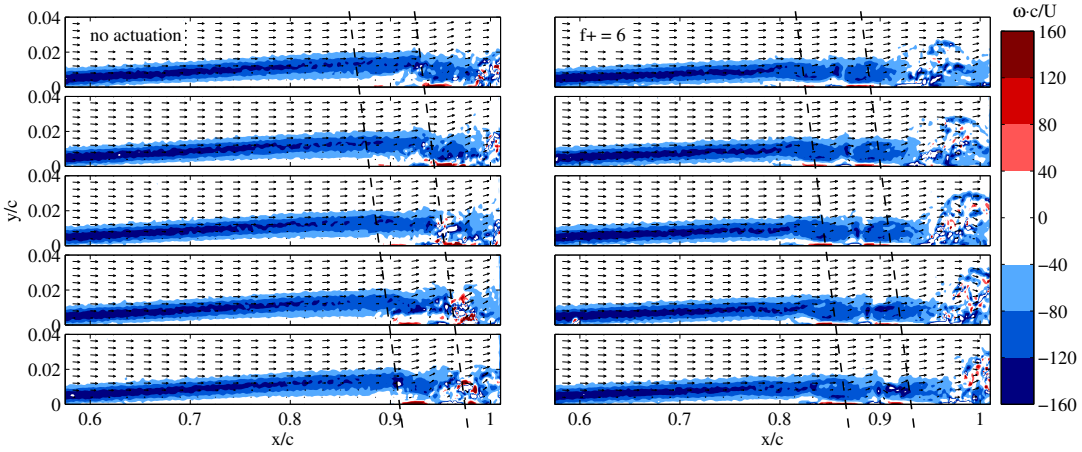

Figure 7. Instantaneous contours of spanwise vorticity for baseline and excitation at $f+ = 6$ and A = 3.5 kV_{pp}. Each consecutive snapshot is separated by 0.5 *ms*, and dashed lines trace the approximate streamwise position of separated shear layer vortices.

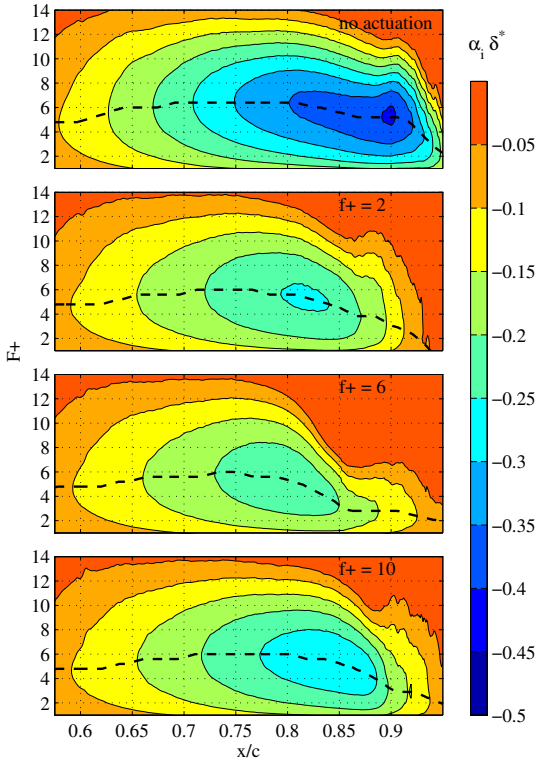

Figure 8. Linear stability curves based on measured mean velocity fields. For the controlled cases, the mean flow fields were acquired with actuator operated at 3.5 kV_{pp}.

Fig. 8 presents contours of the local growth rate of disturbances (α_i). Note that the results of stability analysis can be expected to provide reasonable predictions only in the fore portion of the separation bubble, until the amplified disturbances reach significant amplitudes. The results pertaining to the baseline case agree well with the measured data. Specifically, past separation (x/c = 0.62), the highest growth rate (i.e., lowest α_i values) is associated with disturbances whose frequency $F+ \approx 6$, agreeing with the spectral results in Fig.6. When excitation is applied at $f+ = 2$, 6, and 10, separation occurs at $x/c \approx 0.65$, 0.68, and 0.65, respectively (Fig.4). At and immediately downstream of these locations, the frequency associated with the highest growth rates remains close to the frequency of the most amplified disturbances in the undisturbed separation bubble ($F+ \approx 6$). This is quite remarkable considering that the maximum vertical and streamwise extend of the separation bubble decreases by approximately a factor of two. The implication here is that the mean flow deformation induced by controlled local flow excitation does not significantly affect the frequency of the most amplified disturbances in a separation bubble. This conclusion is supported by the results of Yarusevych *et al.* (2006), where optimal frequency of acoustic excitation matched the fundamental frequency in the unexcited flow to within about 10% for the majority of the cases examined. Moreover, considering recent numeric results of Marxen *et al.* (2015), the variations observed in the frequency associated with the most amplified disturbances in a separation bubble is also relatively minor compared to the deformation of the degree of deformation of the mean bubble induced by the simulated synthetic jet actuation. It should be noted that in all of these cases, including the present study, the mean flow deformation in the separation bubble is induced by the introduction of relatively low amplitude periodic disturbances. These lead to mean flow deformation by promoting separated shear layer transition rather by directly modifying the flow field. In contrast, stronger flow control devices that inject significant momentum may produce flow deformations that will lead to more substantial changes in stability characteristics.

CONCLUSIONS

The effect of controlled local disturbances on flow development and stability of a laminar separation bubble has been investigated experimentally on a NACA 0012 airfoil at $\alpha = 2^\circ$ and Re_c = 130,000. The disturbances were introduced upstream of separation by means of a surface-mounted DBD plasma actuator. The results demonstrate that the introduction of periodic disturbances leads to the reduction in the size of the separation bubble. The most significant effect is produced when excitation is applied at

the frequency matching the frequency of the most amplified disturbances in baseline flow, i.e., the fundamental frequency. The introduced disturbances and their harmonics and a sub harmonic are amplified in the separated shear layer, with the strongest amplification occurring at the fundamental frequency. This promotes transition, leading to earlier reattachment, and increasing the amplitude of the introduced disturbances enhances this effect. In addition to inducing earlier transition, boundary layer separation is also delayed, leading to the overall reduction in the extent of the separation bubble.

The amplification of disturbances in the separated shear layer eventually leads to shear layer roll-up and shedding of vortices at the frequency matching that of the most amplified disturbances. When the excitation is applied, the roll-up occurs earlier and shedding becomes more coherent. The produced structures entrain higher-momentum fluid and lead to local flow reattachment, whose location varies with shedding cycle.

The linear stability theory analysis has showed good agreement with experimental measurements. The results demonstrate that significant mean flow deformation produced due to the introduction of controlled disturbances does not significantly affect the frequency of the most amplified disturbances in the separated shear layer. This finding, however, is speculated to be applicable only to the cases when the control method itself does not directly produce significant changes to the mean flow field.

ACKNOWLEDGEMENT

The authors gratefully acknowledge the Natural Sciences and Engineering Research Council of Canada (NSERC Discovery Grant #112539) and TU Delft for funding this work.

REFERENCES

Alam, M. & Sandham, N. D. 2000 Direct numerical simulation of 'short' laminar separation bubbles with turbulent reattachment. *Journal of Fluid Mechanics* **410**, 1–28.

Boutilier, M. S. H. & Yarusevych, S. 2012 Separated shear layer transition over an airfoil at a low reynolds number. *Physics of Fluids* **24** (8).

Burgmann, S. & Schroeder, W. 2008 Investigation of the vortex induced unsteadiness of a separation bubble via time-resolved and scanning piv measurements. *Experiments in Fluids* **45** (4), 675–691.

Carmichael, B.H. 1981 Low reynolds number airfoil survey. NASA Contract Report No.165803, Vol.1.

Dovgal, A. V., Kozlov, V. V. & Michalke, A. 1994 Laminar boundary layer separation: Instability and associated phenomena. *Progress in Aerospace Sciences* **30** (1), 61–94.

Gaster, M. 1967 The structure and behaviour of laminar separation bubbles. *Reports and Memoranda No. 3595, Aeronautical Research Council, London* .

Greenblatt, D. & Wygnanski, I. J. 2000 Control of flow separation by periodic excitation. *Progress in Aerospace Sciences* **36** (7), 487–545.

Hain, R., Kähler, C. J. & Radespiel, R. 2009 Dynamics of laminar separation bubbles at low-reynolds-number aerofoils. *Journal of Fluid Mechanics* **630**, 129–153.

Gad-el Hak, M. 2001 Flow control: The future. *Journal of Aircraft* **38** (3), 402–418.

Jones, L. E., Sandberg, R. D. & Sandham, N. D. 2010 Stability and receptivity characteristics of a laminar separation bubble on an aerofoil. *Journal of Fluid Mechanics* **648**, 257–296.

Kotsonis, M. & Ghaemi, S. 2011 Forcing mechanisms of dielectric barrier discharge plasma actuators at carrier frequency of 625 hz. *Journal of Applied Physics* **110** (11).

Marxen, O. & Henningson, D. S. 2011 The effect of small-amplitude convective disturbances on the size and bursting of a laminar separation bubble. *Journal of Fluid Mechanics* **671**, 1–33.

Marxen, O., Kotapati, R. B., Mittal, R. & Zaki, T. 2015 Stability analysis of separated flows subject to control by zero-net-mass-flux jet. *Physics of Fluids* **27** (2).

Marxen, O., Lang, M. & Rist, U. 2013 Vortex formation and vortex breakup in a laminar separation bubble. *Journal of Fluid Mechanics* **728**, 58–90.

Postl, D., Balzer, W. & Fasel, H. F. 2011 Control of laminar separation using pulsed vortex generator jets: Direct numerical simulations. *Journal of Fluid Mechanics* **676**, 81–109.

Pröbsting, S., Serpieri, J. & Scarano, F. 2014 Experimental investigation of aerofoil tonal noise generation. *Journal of Fluid Mechanics* **747** (2), 656–687.

Rizzetta, D. P. & Visbal, M. R. 2011 Numerical investigation of plasma-based control for low-reynolds-number airfoil flows. *AIAA Journal* **49** (2), 411–425.

Tani, I. 1964 Low-speed flows involving bubble separations. *Progress in Aerospace Sciences* **5** (C), 70–103.

Van Ingen, J. & Kotsonis, M. 2011 A two-parameter method for en transition prediction. In *6th AIAA Theoretical Fluid Mechanics Conference*.

Yarusevych, S., Kawall, J. G. & Sullivan, P. E. 2006 Airfoil performance at low reynolds numbers in the presence of periodic disturbances. *Journal of Fluids Engineering, Transactions of the ASME* **128** (3), 587–595.

Yarusevych, S., Sullivan, P. E. & Kawall, J. G. 2007 Effect of acoustic excitation amplitude on airfoil boundary layer and wake development. *AIAA Journal* **45** (4), 760–771.